



Article

Self-Cleaning Properties of Electrospun PVA/TiO₂ and PVA/ZnO Nanofibers Composites

Muhammad Qamar Khan ¹, Davood Kharaghani ¹ , Sana Ullah ¹, Muhammad Waqas ², Abdul Malik Rehan Abbasi ³, Yusuke Saito ¹, Chunhong Zhu ⁴ and Ick Soo Kim ^{1,*}

¹ Nano Fusion Technology Research Group, Division of Frontier Fibers, Institute for Fiber Engineering IFES- Interdisciplinary Cluster for Cutting Edge Research ICCER, Shinshu University, Tokida 3-15-1, Ueda, Nagano 386-8567, Japan; qamarkhan154@gmail.com (M.Q.K.); kharaghani66@gmail.com (D.K.); Sanamalik269@gmail.com (S.U.); 15f2020e@shinshu-u.ac.jp (Y.S.)

² Faculty of Textile Engineering, National Textile University, Sheikhpura Road, Faisalabad 37610, Pakistan; waqaskashmiri58@gmail.com

³ Department of Textile Engineering, Faculty of Engineering, BUIITEMS, Quetta 87300, Pakistan; rehan_abbaci@yahoo.com

⁴ Faculty of Textile Science and Technology, Shinshu University, Ueda Campus 386-8567, Japan; zhu@shinshu-u.ac.jp

* Correspondence: kim@shinshu-u.ac.jp; Tel.: +81-268-215-439

Received: 31 July 2018; Accepted: 19 August 2018; Published: 22 August 2018



Abstract: In this report, polyvinyl alcohol/zinnoxide (PVA/ZnO) & polyvinyl alcohol/titanium dioxide (PVA/TiO₂) nanofibers were manufactured in three different concentrations of ZnO and TiO₂ NPs for the application of self-cleaning properties because metallic oxides, specifically ZnO & TiO₂, have the properties to remove the contaminants by hydroxyl radical (OH⁻¹), which degrades the contaminants into small molecules and finally into CO₂ and H₂O. Therefore, these composites were manufactured by electrospinning. The resultant nanofibers were characterized for morphology by scan electron microscopy (SEM) & transmission electron microscopy (TEM), chemical interactions by Fourier-transform infrared (FT-IR) spectra, crystalline structure by X-ray diffraction (XRD) spectra water absorbency was evaluated by water contact angle, self-cleaning by solar simulator, and thermal degradation was done by thermogravimetric analysis (TGA) for the sake of nanoparticles the content. On the base of the characterization results it was concluded that these PVA/ZnO & PVA/TiO₂ nanofibers have self cleaning properties, but PVA/ZnO nanofibers have higher self-cleaning properties than PVA/TiO₂ nanofibers because PVA/ZnO nanofibers have 95% self-cleaning properties, which is higher than PVA/TiO₂ nanofibers.

Keywords: TiO₂ & ZnO nanoparticles; PVA; self-cleaning; electrospinning; composite

1. Introduction

In recent times nanofibres have been researched and studied widely because of their unique properties and applications [1]. Particularly, their high surface areas to volume ratio, large length to diameter ratio, and light weightiness have made them suitable for a number of applications [2]. They are widely used for filtration, drug delivery [3], tissue engineering, and sensors application in protective clothing for protection against biological and chemical hazards, food processing, and in microelectronics [4,5]. A number of methods for the production of nanofibers are being used, such as self-assembly, drawing, phase separation, and electrospinning [2]. Among these techniques electorspinning is more versatile due to its simple assembly and ease of production of continuous fibers [1,6].

There are a number of ways through which a self-cleaning property can be imparted to nanofibers [7]. Generally, in macro materials two basic methods that are used to develop self-cleaning surfaces are complete hydrophobization or hydrophilization of a surface. In the case of hydrophobic surfaces, water takes away the dust particles and containments that are on the material surface, which has no adhesion because of a reduced wet ability also known as the lotus leaf effect [8,9]. While in case of hydrophilic surfaces developed by coating with semiconducting metal oxides dust, grease and organic containments decompose on exposure to light and are easily taken away by water or rain [10–12]. Use of photo-catalytic metallic oxides to develop hydrophilic self-cleaning surfaces is well known. When a photo-catalytic surface is exposed to light of suitable energy it causes the transition of the electrons from the valence band to the conduction band, leaving behind a hole that can react with water to produce hydroxyl radical. Both the hole and hydroxyl radical have very high oxidative power and can destroy organic matters and air pollutants [11].

To develop a nanofiber based photo-catalytic self-cleaning surface nanocomposite is the best option. Polymeric nanocomposites are unique structures that combine the properties of polymers and filler materials and provide improved properties compared to virgin materials [13]. TiO_2 and ZnO photo-catalysts are being widely used in a number of applications to remove environmental pollutants because of their excellent photo catalytic efficiency and non-toxicity [14,15]. TiO_2 coated on carbon nanotubes can be used to remove environmental pollutants and to kill microorganisms [16]. ZnO nano particles embedded poly (1,4-cyclohexanedimethylene isosorbide terephthalate) fibers show excellent self-cleaning property [17]. If two exciting photo-catalysts, TiO_2 and ZnO , are embedded in a suitable polymer solution, then the resultant composite can effectively be used in a number of applications to destroy organic pollutants. In the literature no work is reported regarding the self-cleaning behavior of ZnO and TiO_2 embedded electrospun PVA nanofibers.

Therefore, in this work we have intended to explore the self-cleaning properties of ZnO and TiO_2 embedded PVA nanofibers. The use of the economical polymer, PVA, as a base material to develop TiO_2 -PVA and ZnO -PVA nano-composites makes them particularly useful for commercial applications. The resultant nanofibers were characterized by Fourier-Transform Infrared Spectroscopy (FT-IR). For the sake of chemical investigation, scanning electron microscope (SEM) was done to investigate the surface morphology, transmission electron microscope (TEM) was done to investigate the dispersion of nanoparticles, and photo-catalytic activity was done to check the self-cleaning properties of the nanofibers.

2. Materials and Methods

2.1. Materials

ZnO and TiO_2 nanoparticles (NPs) were purchased from the Sigma-Aldrich Corporation (Louis, MO, USA), with a dispersion concentration of 50.1 wt % and the size of particles was 50 nm. Methylene blue (powder form, soluble 4 mg/4 mL, was purchased from the Sigma-Aldrich Corporation (Louis, MO, USA). Poly vinyl alcohol (MW: 85,000–124,000, 87–89% hydrolyzed) was purchased from the Sigma-Aldrich Corporation (Louis, MO, USA). Glutaraldehyde (GA, 50% in aqueous solution) was purchased from MP Biomedical (Tokyo, Japan).

2.2. Method

PVA 10% by weight was dissolved in de-ionized H_2O at 60 °C and stirred for 12 h. Glutaraldehyde was added in the solution at 2.5 wt % for cross-linking of the solution. Nanoparticle suspensions of ZnO & TiO_2 were separately embedded in that PVA solution to fabricate the PVA/ ZnO and PVA/ TiO_2 nanofibers. For the fabrication of PVA/ ZnO nanofibers three different concentrations; 5 wt %, 7 wt % and 9 wt % of ZnO nanoparticles were blended with PVA solution by stirring for 5 h and similarly to fabricate the PVA/ TiO_2 nanofibers, TiO_2 nanoparticles in three different concentrations, 5 wt %, 7 wt %, and 9 wt %, were blended with PVA solution by stirring for 5 h. The electrospinning of PVA/ ZnO

and PVA/TiO₂ solutions was done as the solution was loaded in the plastic syringe with an inner diameter of 0.60 mm, in which a Cu electrode was adjusted. The distance from capillary tip to collector was 15 cm and the supply of voltage was 12 kV. The PVA, PVA/ZnO, and PVA/TiO₂ nanofibers were formed without beads at room temperature and at 45% humidity. The resultant nanofibers were cross linked to form nanofibers that are water resistant yet can absorb water but are not soluble in water. The illustration scheme of cross-linking is shown in Figure 1. The hydrochloric acid (HCL) foaming of PVA/ZnO/GA & PVA/TiO₂/GA was done at 30 °C for 60 s. In this reaction, GA and HCl acted as a chemical cross-linking agent and a catalyst, respectively. To enhance the crystalline structure and for stable cross-linking, the PVA/ZnO nanofibers were kept at −20 °C for 3 h, which was followed by thawing at 15 °C for 3 h. This process was repeated three times and the resultant nanofibers were dried at room temperature for 24 h, and then estimated.

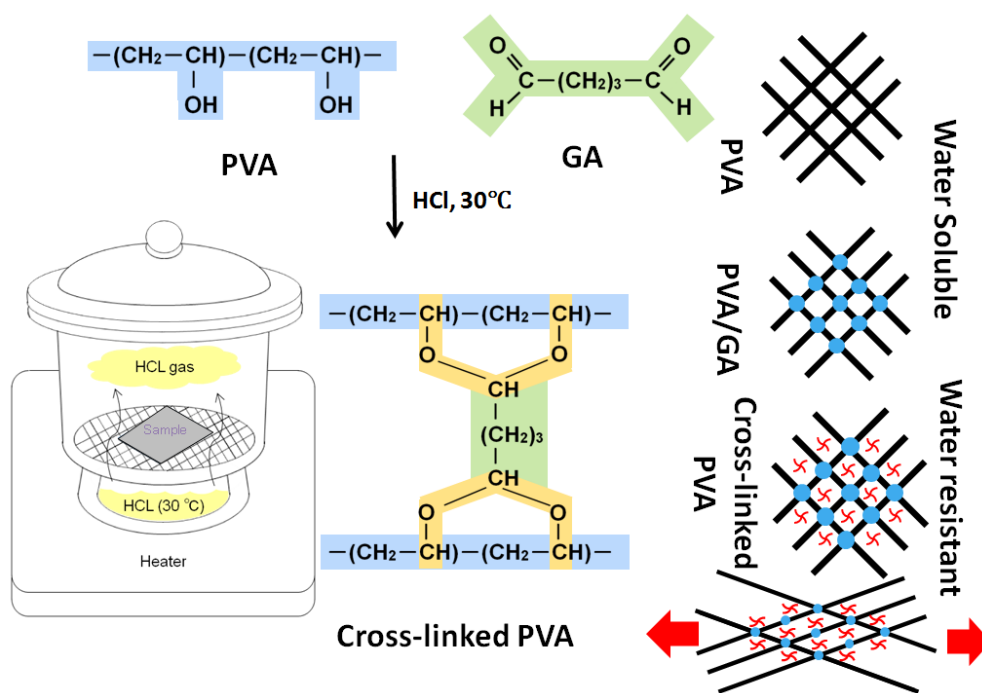


Figure 1. Illustration scheme of cross-linking nanofibers.

2.3. Characterizations

The morphology of the PVA, PVA/ZnO, and PVA/TiO₂ nanofibers was investigated by scan electron microscopy (SEM) (JSM-5300, JEOL Ltd., Tokyo, Japan) accelerated with voltage of 12 kV and transmission electron microscopy (TEM) (JSM-5300, JEOL Ltd., Tokyo, Japan) accelerated with 200 kV. The chemical interactions were studied by FT-IR (IR Prestige-21 by shinmadzu, Nagano, Japan), Wide angle X-ray diffractions (WAXD) spectra were performed for the evaluation of the crystal structure at 25 °C with nanofiber samples using a Rotaflex RT300 mA (Rigaku manufacturer, Osaka, Japan) and Nickel-filtered Cu. Ka radiation was used for measurements, along with an angular angle of $5 \leq 2\theta \leq 50^\circ$. Photo-catalytic activity was done by a solar simulator (XES-40S3, San-ei Electric, Nagano, Japan), stress-strain behavior was studied by a tensile strength tester (Universal Testing Machine, Tenilon RTC 250 A, A &D company Ltd., Tokyo, Japan), water contact angle measurements were done by a contact angle meter (Digidrop, GBX, Whitestone way, France) and photo-catalytic activity was done by a solar simulator (XES-40S3, San-ei Electric, Nagano, Japan). The light intensity was 1000 W/m², the wavelength range was 350–1100 nm, and the self-cleaning efficiency was calculated as the following Equation (1).

$$\text{Degradation (\%)} = \frac{I_i - I_d}{I_i} \times 100 \quad (1)$$

Thermal degradation of PVA, PVA/ZnO & PVA/TiO₂ was performed by thermogravimetric analysis. This thermogravimetric analysis was performed on the thermo-plus TG 8120 (Rigaku Corporation, Osaka, Japan). It was operating in a static mode under air atmosphere at a heating rate of 10 °C/min and a temperature range of 0–700 °C.

3. Results and Discussion

3.1. Morphology of Nanofibers

In order to investigate the surface morphology of nanofibers, SEM images were analyzed as mentioned in Figure 2. All PVA, PVA/ZnO, and PVA/TiO₂ nanofibers were bead free and PVA/ZnO and PVA/TiO₂ nanofibers showed that the blending of the nanoparticles did not affect the surface morphology of the PVA nanofibers as mentioned in Figure 2b–g. It was also analyzed that both ZnO and TiO₂ nanoparticles did not change the surface morphology of the PVA nanofibers. Both nanoparticles affected the size of the nanofibers. When the concentration of nanoparticles was increased, the size of the nanofibers was also increased, as shown in Figure 2b–g.

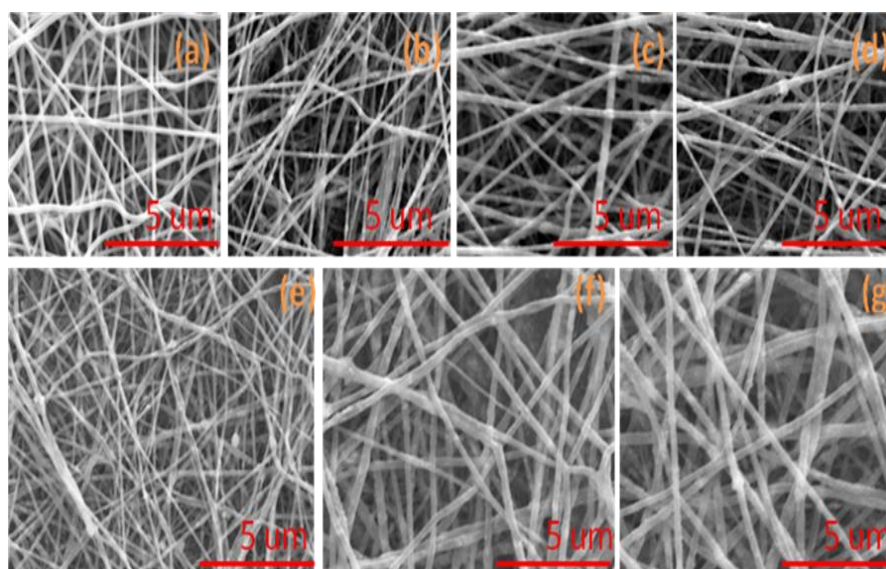


Figure 2. Scanning electron microscope (SEM) images of (a) Neat PVA nanofibers; (b) 5% PVA/ZnO nanofibers; (c) 7% PVA/ZnO nanofibers; (d) 9% PVA/ZnO nanofibers; (e) 5% PVA/TiO₂ nanofibers; (f) 7% PVA/TiO₂ nanofibers; (g) 9% PVA/TiO₂ nanofibers.

In order to investigate the effect of ZnO & TiO₂ nanoparticles on the average diameter of the PVA nanofibers, distribution graphs were studied, as shown in Figure 3. It was analyzed that the average diameter of PVA/ZnO and PVA/TiO₂ was affected by the blending of ZnO & TiO₂ nanoparticles. The average diameter of neat PVA nanofibers was 350 ± 10 nm but the average diameter of PVA/ZnO nanofibers was increased as the concentration of ZnO NPs was increased as mentioned in Figure 3b–d; 5%, 7% & 9% PVA/ZnO nanofibers have an average diameter of 380 ± 15 , 385 ± 20 , and 410 ± 10 nm, respectively. The average diameter of PVA/TiO₂ nanofibers was also increased when the concentration of TiO₂ was increased, as mentioned in Figure 3e–g; 5%, 7% & 9% PVA/TiO₂ nanofibers have an average diameter of 383 ± 05 , 390 ± 10 and 418 ± 15 nm, respectively. It showed that PVA/TiO₂ nanofibers have a greater average diameter than the PVA & PVA/ZnO nanofibers. It also means that the TiO₂ NPs have a greater effect on the PVA nanofibers than ZnO NPs.

In order to investigate the dispersion of the ZnO and TiO₂ nanoparticles on the PVA nanofibers, TEM images were analyzed, as shown in Figure 4. It was analyzed that there was uniform and well dispersion of both the ZnO and TiO₂ nanoparticles on the PVA nanofibers. TEM images also showed

that when the concentrations of nanoparticles were increased, then the diameters of PVA/ZnO and PVA/TiO₂ were also increased. When the concentration of NPs was increased the dispersion of NPs on PVA nanofibers also was increased, as mentioned in Figure 4.

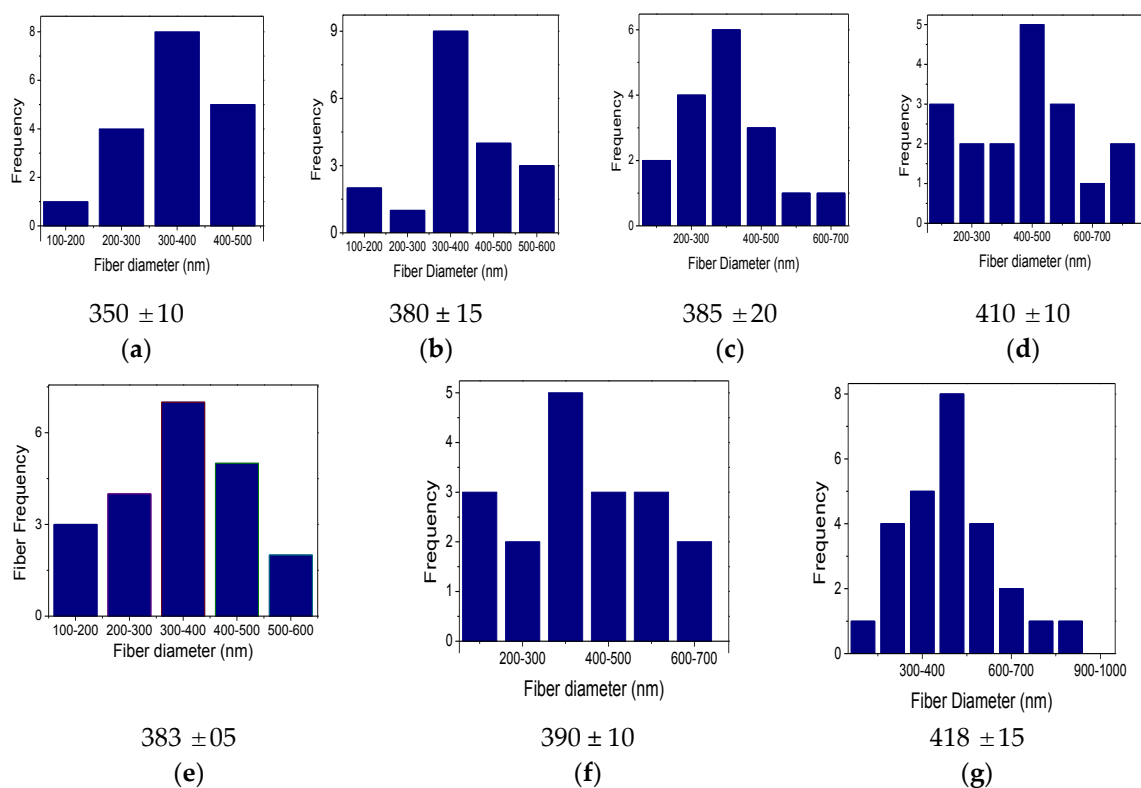


Figure 3. Average diameter distributions analysis of (a) Neat PVA nanofibers; (b) 5% PVA/ZnO nanofibers; (c) 7% PVA/ZnO nanofibers; (d) 9% PVA/ZnO nanofibers; (e) 5% PVA/TiO₂ nanofibers; (f) 7% PVA/TiO₂ nanofibers; (g) 9% PVA/TiO₂ nanofibers.

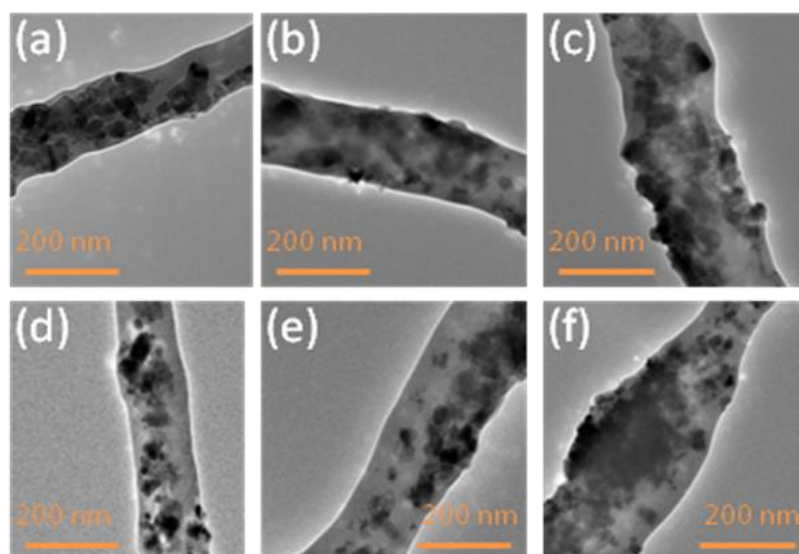


Figure 4. Transmission electron microscope (TEM) analysis of (a) 5% PVA/ZnO nanofibers; (b) 7% PVA/ZnO nanofibers; (c) 9% PVA/ZnO nanofibers; (d) 5% PVA/TiO₂ nanofibers; (e) 7% PVA/TiO₂ nanofibers; (f) 9% PVA/TiO₂ nanofibers.

3.2. Chemical Structure Analysis

In order to investigate the chemical structure analysis of PVA, PVA/ZnO, and PVA/TiO₂ nanofibers, ATR-FTIR spectra were studied, as shown in Figure 5. It was analyzed that there were successful chemical interactions of functional groups between PVA and ZnO & TiO₂ NPs, as shown in Figure 5b–g. The spectra showed that in the neat PVA nanofibers, the bands at about 3320, 2940, 1437, 1093, and 850 cm⁻¹ showed the vibrations of –OH, –CH₂CH, C–C & C–O functional groups of PVA, respectively [18]. The new intense broad bands at 1100 cm⁻¹ to 1000 cm⁻¹ and 750 cm⁻¹ are assigned to metal oxide of the of Zn & Ti, because these oxides have a moderate dipole moment. The oxides of Zn & Ti with more than one oxygen atom bound to a single metal atom usually absorb in the region 1100 to 750 cm⁻¹. In this spectra of PVA/ZnO and PVA/TiO₂, it was shown that O–H bending at 1579 cm⁻¹ and O–H stretching at 3320 cm⁻¹ occurred, which was due to the –O bonding of TiO₂ & ZnO with the –H of PVA. There was stretching vibration of –O of TiO₂ & ZnO with –C and –O of PVA at 1050 and 850 cm⁻¹, respectively, as shown in Figure 5 [19–21]. Therefore, these spectra confirmed that this self cleaning composite was composed with PVA/ZnO and PVA/TiO₂.

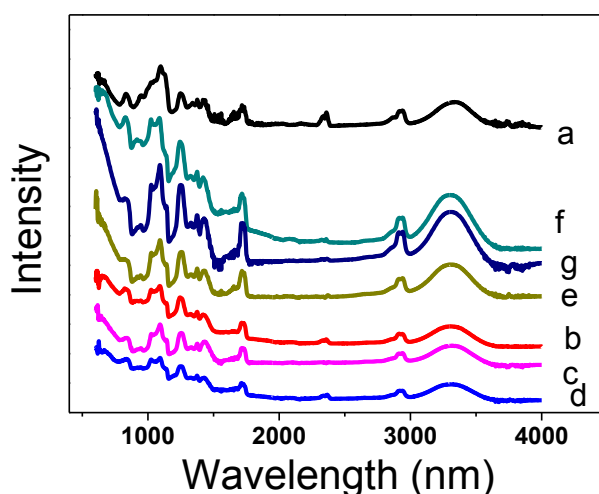


Figure 5. Fourier-transform infrared (FTIR) spectra of (a) Neat PVA nanofibers; (b) 5% PVA/ZnO nanofibers; (c) 7% PVA/ZnO nanofibers; (d) 9% PVA/ZnO nanofibers; (e) 5% PVA/TiO₂ nanofibers; (f) 7% PVA/TiO₂ nanofibers; (g) 9% PVA/TiO₂ nanofibers.

3.3. XRD Study

In order to investigate the crystalline structure of PVA, PVA/ZnO and PVA/TiO₂ nanofibers XRD spectra were studied, as shown in Figure 6. It was analyzed that the crystallinity of the PVA nanofibers was affected by blending the nanoparticles of ZnO and TiO₂, but ZnO NPs had a greater effect than TiO₂ NPs, as shown in Figure 6. PVA/ZnO nanofibers have a greater crystalline structure than PVA & PVA/TiO₂ nanofibers. 9% by weight ZnO/PVA nanofibers have a higher crystalline structure than other 7% & 5% by weight ZnO/PVA nanofibers, which exhibit the peak at 18°, 29°, 31° & 34° with high intensity, 7% & 5% by weight ZnO/PVA nanofibers exhibit the peak at 18°, 29°, 31° & 34° with low intensity than 9% by weight ZnO/PVA nanofibers. 9% by weight TiO₂/PVA nanofibers exhibit the peak at 18°, 20° and 36° with high intensity than 5% & 7% by weight of TiO₂/PVA nanofibers but 5% by weight of TiO₂/PVA nanofibers did not show the crystalline structure at 36° [15,19]. Therefore, due to cross-linking, the crystalline structure of PVA/ZnO & PVA/TiO₂ was increased. This crystalline structure made them water resistant nanofibers.

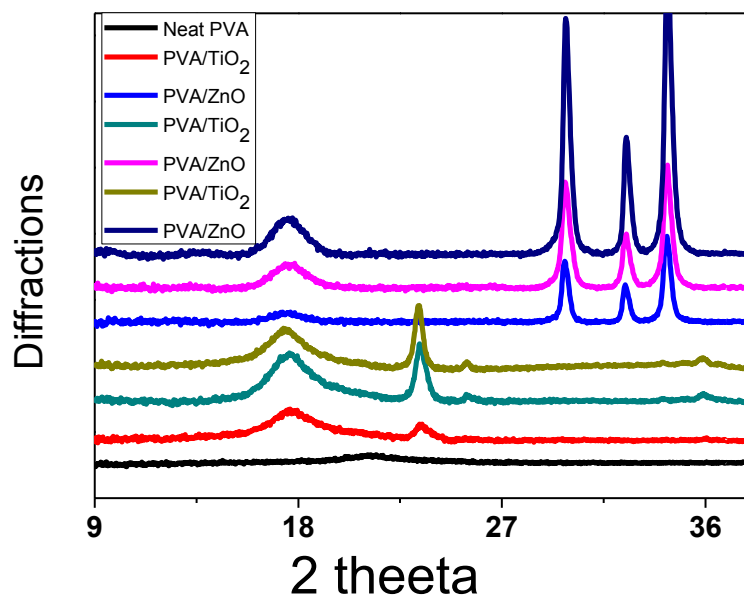


Figure 6. X-ray diffraction (XRD) spectra of Neat PVA nanofibers and PVA/ZnO nanofibers.

3.4. Water Contact Angle Measurements

In order to investigate the wetting behavior of PVA, PVA/ZnO and PVA/TiO₂ nanofibers, water contact angle measurements were studied, as shown in Figure 7. It was analyzed that when crystallinity of PVA/ZnO & PVA/TiO₂ nanofibers was increased, the capacity of water absorbency was reduced. Therefore, these nanofibers showed more water contact angle values than neat PVA nanofibers, as mentioned in Figure 7. It was also analyzed that when the concentration of both ZnO and TiO₂ NPs was increased the water contact angle's value was increased, but TiO₂ NPs has a greater effect than ZnO NPs, as mentioned in Figure 7.

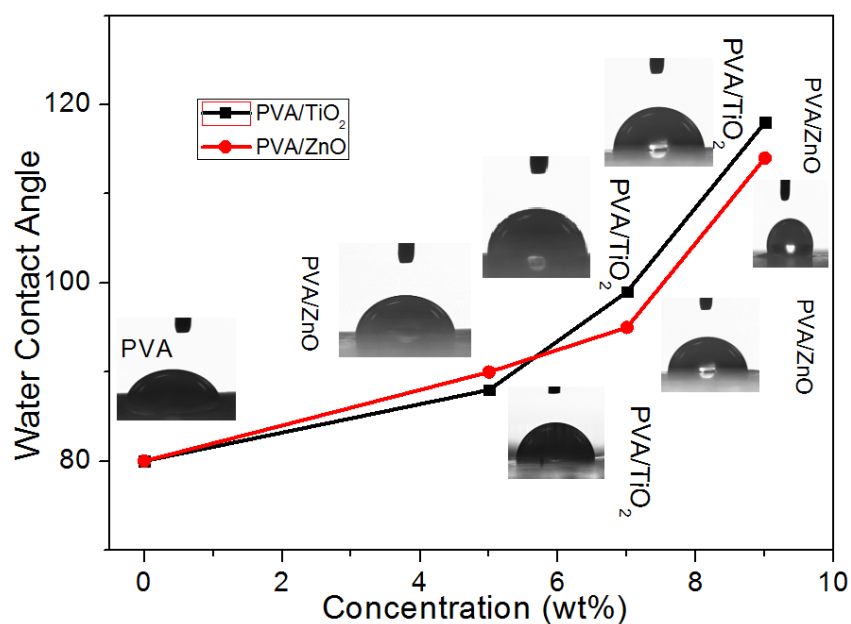


Figure 7. Wetting behavior of Neat PVA nanofibers; 5% PVA/ZnO nanofibers; 7% PVA/ZnO nanofibers; 9% PVA/ZnO nanofibers; 5% PVA/TiO₂ nanofibers; 7% PVA/TiO₂ nanofibers; 9% PVA/TiO₂ nanofibers.

3.4.1. Photo-Catalysis Study

In order to investigate the self-cleaning efficiency of PVA, PVA/ZnO and PVA/TiO₂ nanofibers, a photo-catalysis study was conducted by solar simulator with a light intensity of 1000 W/m² and a wavelength range of 350–1100 nm. In this activity, the photo-catalyst absorbs the UV light, which convert the H₂O into hydroxyl radical (OH⁻¹), which degrades the contaminants into small molecules and finally into CO₂ and H₂O [17]. The objective of this research was to develop the self-cleaning nanocomposites in two different ways: PVA/ZnO and PVA/TiO₂ nanofibers. Three different concentrations, 5%, 7% & 9% by weight, of ZnO and TiO₂ NPs were separately blended in PVA nanofibers, but the self-cleaning comparison of both was analyzed at 9% by weight PVA/ZnO and PVA/TiO₂ nanofibers, as shown in Figure 8. Methylene blue (MB) dye was used for analyzing the self-cleaning properties of these composites. 2 μL MB was dropped on each sample of PVA, PVA/ZnO & PVA/TiO₂ nanofibers. It was observed that there was no self-cleaning property in PVA but PVA/ZnO and PVA/TiO₂ nanofibers have self-cleaning properties, as mentioned in Figure 8. The comparative study between PVA/ZnO and PVA/TiO₂ nanofibers was done in two ways; first by the naked eye, as shown in Figure 8A, and second by ATR spectra, in which the intensity of the methylene blue was measured by using Equation (2).

$$\text{Degradation (\%)} = \frac{I_i - I_d}{I_i} \times 100 \quad (2)$$

where I_i is the initial intensity of dyed nanofibers and I_d is the degraded intensity of dyed nanofibers. Therefore, degradation efficiency/percentage was calculated from ATR spectra, which showed that PVA/ZnO nanofibers have a higher self-cleaning efficiency than PVA/TiO₂ nanofibers because PVA/ZnO nanofibers showed a 95% self-cleaning efficiency within three hours but the PVA/TiO₂ nanofibers showed less efficiency than the PVA/ZnO nanofibers, as shown in Figure 8b,c.

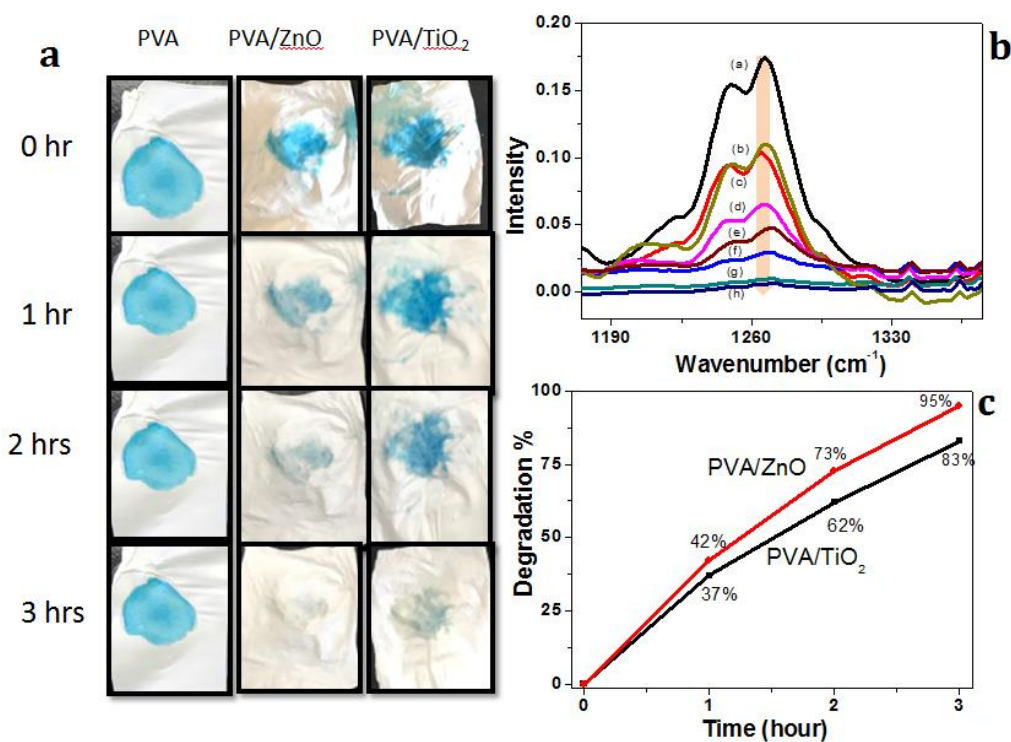


Figure 8. Photo-catalysis efficiency in 3 h of neat PVA nanofibers, 9% PVA/ZnO nanofibers and 9% PVA/TiO₂ nanofibers, (a) photocatalytic activity by solar simulator; (b) Self-cleaning efficiency calculated by FT-IR; (c) profile of self cleaning efficiency of PVA/ZnO & PVA/TiO₂.

3.4.2. Thermogravimetric Analysis (TGA)

Thermal degradation of PVA, PVA/ZnO & PVA/TiO₂ was performed by thermogravimetric analysis as shown in Figure 9. This thermogravimetric analysis was performed on the thermo-plus TG 8120 Rigaku Corporation Japan. It was operating in a static mode under air atmosphere at a heating rate of 10 °C/min and a temperature range from 30–500 °C. The samples weighing 6 mg were placed in the pans. The TGA curves of neat PVA, PVA/TiO₂ and PVA/ZnO nanofibers as shown in Figure 9 showed that PVA/TiO₂ & PVA/ZnO showed the same thermal stability as neat PVA nanofibers. In this test PVA nanofibers did show smaller residual mass than PVA/TiO₂ & PVA/ZnO nanofibers. The PVA/TiO₂ & PVA/ZnO nanofibers showed the residual mass that confirmed the presence of nanoparticles of ZnO and TiO₂ as shown in the Figure 9. The neat PVA showed 93% degradation at 470 °C, but 5 wt % PVA/ZnO showed 73%, 7 wt % PVA/ZnO 64%, and 9 wt % PVA/ZnO 61% showed degradation, which confirmed that there was a good amount of ZnO nanoparticles. Similarly, PVA/TiO₂ also showed less degradation than PVA, which confirmed the presence of TiO₂ nanoparticles in the PVA/TiO₂ as shown in Figure 9B [22,23].

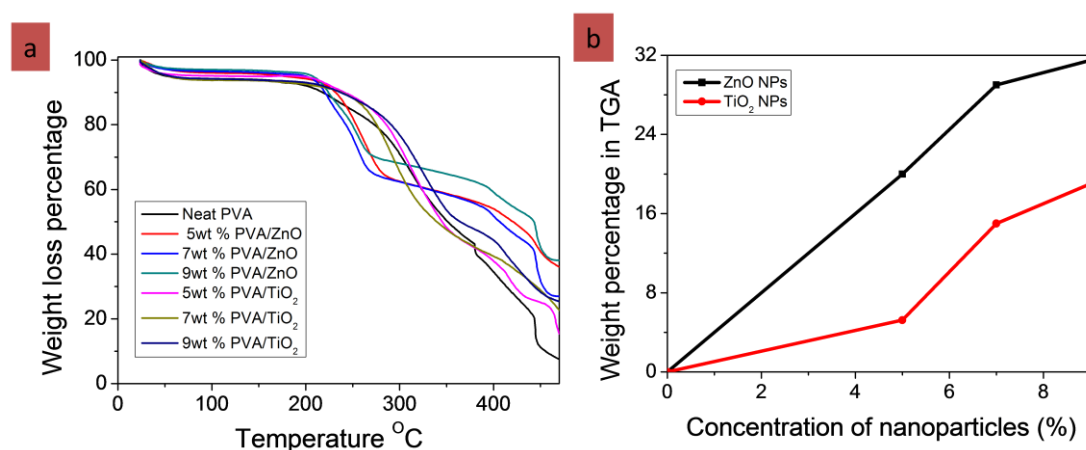


Figure 9. Results of TGA (a) showed the degradation behavior; (b) content percentage of ZnO and TiO₂ NPs in 6 mg of sample.

4. Conclusions

Herein, we successfully developed self-cleaning PVA/ZnO & PVA/TiO₂ nanofibers by electrospinning in three different concentrations of ZnO and TiO₂ NPs. On the basis of the characterization results, it was concluded that these PVA/ZnO & PVA/TiO₂ nanofibers have self-cleaning properties, but PVA/ZnO nanofibers have higher self-cleaning properties than PVA/TiO₂ nanofibers because 9% by weight PVA/ZnO nanofibers has 95% self-cleaning properties, which is higher than 9% by weight PVA/TiO₂ nanofibers. This innovative research is essential to form intelligent textiles for stain eliminating from non-washable & non-woven products, such as surgical gown, wound dressings, and home textiles. This research will be fruitful to fulfill the stated and implied needs of customers.

Author Contributions: I.S.K. and C.Z. designed the DOE of the experiment; M.Q.K. did experiment and wrote, D.K., S.U. and Y.S. did characterizations. A.M.R.A. and M.W. did the writing review.

Funding: This research received no external funding.

Acknowledgments: All authors acknowledge the support of Division of Frontier Fibers, Institute for Fiber Engineering (IFES-), for providing the materials and all related characterizations.

Conflicts of Interest: The authors declare no conflict of interest.

References

1. Czado, W.; Frese, T.; Schaper, A.; Hellwig, M.; Steinhart, M.; Greiner, A.; Wendorff, J.H.; Bognitzki, M. Nanostructured Fibers via Electrospinning. *Adv. Mater.* **2001**, *13*, 70–72.
2. Fujihara, K.; Teo, W.-E.; Lim, T.-C.; Ma, Z.; Ramakrishna, S. *An Introduction to Nanofibers and Electrospinning*; World Scientific Publishing Co. Pte. Ltd.: Majulah, Singapore, 2005.
3. Sell, S.A.; Boland, E.D.; Simpson, D.G.; Bowlin, G.L.; Barnes, C.P. Nanofiber technology: Designing the next generation of tissue engineering scaffolds. *Sci. Dir.* **2007**, *59*, 1413–1433.
4. Bhat, G.S.; Tock, R.W.; Parameswaran, S.; Ramkumar, S.S.; Subbiah, T. Electrospinning of Nanofibers. *Wiley InterSci.* **2004**, *96*, 557–569.
5. Wei, Q. *Functional Nanofibers and Their Applications*; Woodhead Publishing: Cambridge, UK, 2012.
6. Kundu, S.C.; Bhardwaj, N. Electrospinning: A fascinating fiber fabrication technique. *Biotechnol. Adv.* **2010**, *28*, 325–347.
7. Bedford, N.M.; Steckl, A.J. Photocatalytic Self Cleaning Textile Fibers by coaxial electrospinning. *Appl. Mater. Interfaces* **2010**, *2*, 2448–2455. [[CrossRef](#)]
8. Lyua, S.; Leea, S.; Kimb, Y.S.; Hwang, W.; Leea, K. Characteristics and self-cleaning effect of the transparent super-hydrophobic film having nanofibers array structures. *Appl. Surf. Sci.* **2010**, *256*, 6729–6735.
9. Tang, J.; Wang, R.; Lu, H.; Li, L.; Kong, Y.; Qi, K.; Xin, J.H.; Liu, Y. Artificial lotus leaf structures from assembling carbon nanotubes and their application in hydrophobic textile. *J. Mater. Chem.* **2007**, *17*, 1071–1078.
10. Guan, K. Relationship between photocatalytic activity, hydrophilicity and self-cleaning effect of TiO₂/SiO₂ films. *Surf. Coat. Technol.* **2005**, *191*, 155–160. [[CrossRef](#)]
11. Dehn, F.; Quaas, J.; Orgass, M.; Benedix, R. Application of Titanium Dioxide Photocatalysis to Create Self-Cleaning Building Materials. In *Leipzig Annual Civil Engineering Report Lacer No. 5*; Univ., Wirtschaftliche Fakultät, Fachgruppe Bau- und Wirtschaftsingenieure: Leipzig, Germany, 2005; pp. 157–167.
12. Zhang, Y.-Z.; Khotki, M.; Ramakrishna, S.; Huang, Z.-M. A review on polymer nanofibers by electrospinning and their applications in nanocomposites. *Compos. Sci. Technol.* **2003**, *63*, 2223–2253.
13. Luo, Z.; Rabenberg, L.; Heller, A.; Paz, Y. Photooxidative self-cleaning transparent titanium dioxide films on glass. *J. Mater. Res.* **1995**, *10*, 2842–2848.
14. Pyrgiotakis, G.; Sigmund, W.; Woan, K. Photocatalytic Carbon-Nanotube-TiO₂ Composites. *Adv. Mater.* **2009**, *21*, 2223–2239.
15. Jiang, X.; Wang, T. Influence of Preparation Method on Morphology and Photocatalysis Activity of Nanostructured TiO₂. *Environ. Sci. Technol.* **2007**, *41*, 4441–4446. [[CrossRef](#)] [[PubMed](#)]
16. Jimmy, C.Y.; Yu, J.-G.; Kwok, Y.-C.; Che, Y.-K.; Zhao, J.-C.; Ding, L.; Ge, W.-K.; Wong, P.-K.; Yu, Y. Enhancement of photocatalytic activity of mesoporous TiO₂ by using carbon nanotubes. *Appl. Catal. A* **2005**, *289*, 186–196.
17. Lee, H.; Koo, J.M.; Khatri, Z.; Sui, J.; Im, S.S.; Zhu, C.; Kim, I.S.; Khan, M.Q. Self-cleaning effect of electrospun poly (1,4-cyclohexanedimethylene isosorbide terephthalate) nanofibers embedded with zinc oxide nanoparticles. *Text. Res. J.* **2017**. [[CrossRef](#)]
18. Kharaghani, D.; Lee, H.; Ishikawa, T.; Nagaiishi, T.; Kim, S.H.; Kim, I.S. Comparison of fabrication methods for the effective loading of Ag onto PVA nanofibers. *Text. Res. J.* **2018**. [[CrossRef](#)]
19. Boyadjiev, S.I.; Kéri, O.; Bárdos, P.; Firkala, T.; Gáber, F.; Nagy, Z.K.; Baji, Z.; Takács, M.; Szilágyi, I.M. TiO₂/ZnO and ZnO/TiO₂ core/shell nanofibers prepared by electrospinning and atomic layer deposition for photocatalysis and gas sensing. *Appl. Surf. Sci.* **2017**, *424*, 190–197. [[CrossRef](#)]
20. Kaviyarasu, K.; Geetha, N.; Kanimozhi, K.; Magdalane, C.M.; Sivaranjani, S.; Ayeshamariam, A.; Kennedy, J.; Maaza, M. In vitro cytotoxicity effect and antibacterial performance of human lung epithelial cells A549 activity of zinc oxide doped TiO₂ nanocrystals: Investigation of bio-medical application by chemical method. *Mater. Sci. Eng. C* **2017**, *74*, 325–333. [[CrossRef](#)] [[PubMed](#)]
21. Boccuzzi, F.; Chiorino, A.; Tsubota, S.; Haruta, M. FTIR study of carbon monoxide oxidation and scrambling at room temperature over gold supported on ZnO and TiO₂. *J. Phys. Chem.* **1996**, *100*, 3625–3631. [[CrossRef](#)]

22. Ognibene, G.; Cristaldi, D.A.; Fiorenza, R.; Blanco, I.; Cicala, G.; Scire, S.; Fragala, M.E. Photoactivity of hierarchically nanostructured ZnO–PES fibre mats for water treatments. *RSC Adv.* **2016**, *6*, 42778–42785. [[CrossRef](#)]
23. Juby, K.A.; Dwivedi, C.; Kumar, M.; Kota, S.; Misra, H.S.; Bajaj, P.N. Silver nanoparticle-loaded PVA/gum acacia hydrogel: Synthesis, characterization and antibacterial study. *Carbohydr. Polym.* **2012**, *89*, 906–913. [[CrossRef](#)] [[PubMed](#)]



© 2018 by the authors. Licensee MDPI, Basel, Switzerland. This article is an open access article distributed under the terms and conditions of the Creative Commons Attribution (CC BY) license (<http://creativecommons.org/licenses/by/4.0/>).